Scattering of polarized and unpolarized neutrons from ^{93}Nb from 8 to 17 MeV and optical model descriptions

R. S. Pedroni,* R. C. Byrd,† G. M. Honoré,‡ C. R. Howell, and R. L. Walter
Department of Physics, Duke University, Durham, North Carolina 27706
and Triangle Universities Nuclear Laboratory, Duke Station, North Carolina 27706
(Received 30 April 1990; revised manuscript received 10 January 1991)

Differential cross sections and analyzing powers for neutron elastic scattering from ^{93}Nb have been measured at energies from 8 to 17 MeV using pulsed-beam time-of-flight methods. These data plus total cross-section data from 1 to 20 MeV are interpreted in terms of the spherical optical model. Several sets of optical potential parameters with systematic energy dependences have been derived in searches that used different initial parameter sets. In addition, comparisons of the data to calculations based on previously reported optical potentials are presented. It is concluded that the data favor the inclusion of a small imaginary spin-orbit term.
MS code no. CR4145 1990 PACS number(s): 25.40.Dn, 24.10.Ht, 24.70.+s

I. INTRODUCTION

In a continuation of the ongoing investigation of 8–17-MeV neutron-nucleus scattering at the Triangle Universities Nuclear Laboratory (TUNL), our program of measurements and analyses has been extended to include the nucleus ^{93}Nb. It was anticipated that descriptions of the elastic-scattering data could proceed successfully with the conventional spherical optical model (SOM). In fact, Lagrange and Lejeune[1] have reported such an analysis of ^{93}Nb$(n,n)^{93}$Nb for several types of observables in the energy range 10 keV to 50 MeV, and the present data provide a test of their model. Measurements in the energy range from 8 to 17 MeV for nuclei near $A=90$ also provide necessary information for developing and testing global nucleon-nucleus scattering models. Such models are useful for basic and applied nuclear physics.

In the present paper differential cross sections $\sigma(\theta)$ are reported for elastic scattering of neutrons from ^{93}Nb at incident energies of 7.95, 9.94, 11.93, 13.92, and 16.91 MeV, and analyzing powers $A_y(\theta)$ are reported at 9.94 and 13.92 MeV. (These data supplement our companion study[2] of neutron scattering from the nucleus ^{89}Y.) For both of the observables, only elastic-scattering data were extracted. In the SOM analyses reported here, the goal was to use the conventional Woods-Saxon form factors for the optical model potential (OMP) and to search for a set of OMP parameters constrained to have systematic energy dependences. Reasonable success was achieved.

A second goal was to use the present data as a test of an existing SOM for ^{93}Nb and of some published nucleon-nucleus global SOM parameter sets. These comparisons, which are presented below, are particularly significant since the present measurements provide the only $A_y(\theta)$ data available above 4 MeV for this nucleus.

Our last aim was to contribute an additional set of $\sigma(\theta)$ and $A_y(\theta)$ data to a large database for developing nucleon-nucleus interaction models that are intended to give consistent predictions for a variety of nuclei over a wide energy range. The most recent report of a global study for neutrons was given by Walter and Guss[3] in 1986; these authors based their study on real and imaginary potentials that have the customary Woods-Saxon form factors. Another global approach can be provided by microscopic models based on effective nucleon-nucleus interactions; the present ^{93}Nb data are being incorporated into such a project conducted by Hansen, Dietrich, and one of the present authors (R.L.W.).[4]

II. EXPERIMENT

A. Data acquisition

Both differential cross sections and analyzing powers were measured using pulsed-beam time-of-flight (TOF) methods, and the data were taken alternately in the same experiment[2] as that for ^{89}Y. The experimental arrangements for such measurements at TUNL have been described in earlier papers.[5,6] In brief, a deuteron beam is pulsed and then accelerated with the FN tandem Van de Graaff, producing a pulsed neutron beam via the ^{2}H$(d,n)^3$He reaction. Neutrons emitted at 0° in the source reaction scatter from a cylindrical target of ^{93}Nb that is 2.71 cm in height and 2.57 cm in diameter and that has a mass of 120 g. The impurities in the target are estimated to be less than 0.5% and believed to be comprised of light elements such as oxygen. Neutrons scattered by the sample are detected by two heavily shielded liquid organic scintillators, positioned at flight paths of approximately 4 and 6 m, respectively. A third neutron detector, which views the source reaction from above the reaction plane, monitors the neutron flux. The system utilized standard TOF electronics, including pulse-shape discrimination to reduce unwanted counts due to γ rays.

In the measurement of $A_y(\theta)$, a pulsed deuteron beam from the TUNL Lamb-shift polarized ion source is used to produce polarized neutrons through the polarization-transfer reaction ^{2}H$(d,n)^3$He at a reaction angle of 0°. The deuteron beam polarization is measured by the quench-ratio method.[7] The vector polarization of the

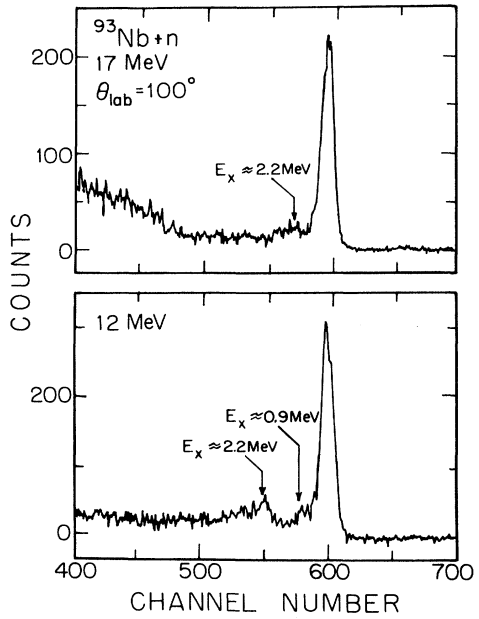

FIG. 1. Time-of-flight spectra for the scattering of 17-MeV (top) and 12-MeV (bottom) unpolarized neutrons from niobium to a laboratory angle of $\theta = 100°$. Flight time increases from right to left. The large peaks correspond to elastic scattering. For calibration purposes, the locations are indicated where states in the vicinity of excitation energies of 0.9 and 2.2 MeV would appear. Note the offset for zero counts.

deuteron beam is typically 70%, producing a neutron beam with a polarization of about 63%. The $A_y(\theta)$ measurements are conducted in the same target area as the $\sigma(\theta)$ measurements and use the same TOF detectors. However, for the $A_y(\theta)$ data, measurements are made with both detectors set simultaneously at equal reaction angles on opposite sides of the incident beam axis. In this way the "two-detector, spin-flip" method[8] can be employed to minimize instrumental asymmetries.

Samples of time-of-flight spectra from $\sigma(\theta)$ measurements are shown in Fig. 1. The spectra for $A_y(\theta)$ measurements are of similar quality. Time of flight increases from right to left. The peak at the far right is due to elastic scattering from ^{93}Nb. The spectra in Fig. 1 are called "difference spectra" and are generated by subtracting "sample-out" spectra (that is, spectra obtained with the sample removed) from the "sample-in" spectra, thereby eliminating sample-uncorrelated background. For the $\sigma(\theta)$ measurements the difference spectra are normalized to the yields in the flux-monitor detector to obtain a relative angular distribution at each energy. These distributions are converted to absolute cross sections by normalizing to yields obtained from neutron scattering from hydrogen and using the well-known n-p scattering cross sections.[9] A polyethylene target was used in the n-p scattering measurements. In the case of the $A_y(\theta)$ measurements, the integrated beam current at the target replaced the flux-monitor yield for purposes of normalization of the "sample-in" and "sample-out" runs. The experimental resolution was not sufficient to extract $\sigma(\theta)$ or $A_y(\theta)$ values for inelastic scattering to discrete states in ^{93}Nb, so only values for elastic scattering were determined. Any yield from inelastic scattering to the first excited state at 0.030 MeV would not be distinguished from elastic scattering. However, as discussed later, the contribution from this inelastic group is negligible.

Corrections were made of the data for effects of finite geometry and multiple scattering, using the TUNL Monte Carlo codes EFFIGY and JANE for correcting the cross-section data[10] and the analyzing power data,[11] respectively. The corrections to the yields were relatively large because the average attenuation of the out-going neutrons in a solid cylindrical sample of the size used in the present measurement is large. This is illustrated in the top half of Fig. 2, where the open circles show the measured yield normalized to the ^{1}H$(n,n)^1$H scattering yield and where the crosses represent the data corrected for the attenuation. The final data, indicated by the solid circles, have been corrected for effects due to multiple scattering in the sample, due to the angular acceptance of the detector, and due to the relatively wide angle subtended by the scattering sample at the neutron source. Applying the overall correction for both of these latter effects results in lowering the minima by a factor of 2 in some cases (see Fig. 2) and in shifting the average measuring angle away from that determined optically from the line of center of the sample and detector. In the lower half of Fig. 2 the uncorrected data (open circles) and corrected data (solid circles) are shown to indicate the magnitude of the correction and the angle shifts produced when the $A_y(\theta)$ data are corrected using the code

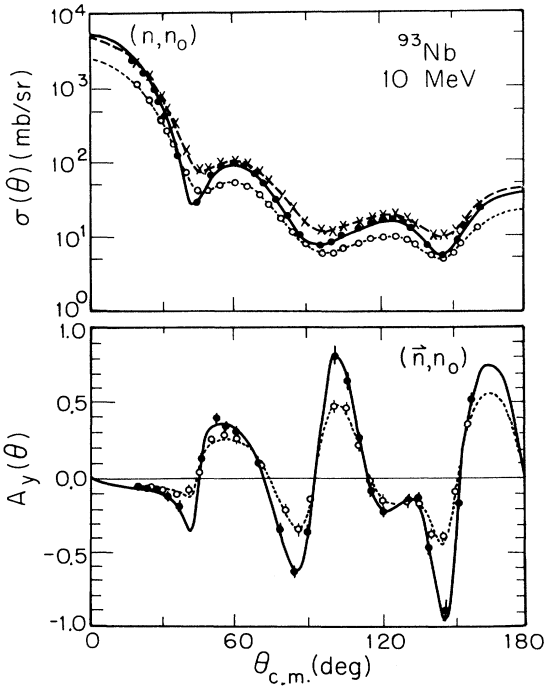

FIG. 2. Illustrations of uncorrected and corrected $\sigma(\theta)$ and $A_y(\theta)$ data for 10 MeV. See text for description.

JANE. The ^{93}Nb target is the largest sample in physical dimensions that we have used in our neutron-scattering studies; therefore the illustrations in Fig. 2 are intended to document some of the "worst-case" corrections.

B. Final data

The final $\sigma(\theta)$ data are shown in Fig. 3. The relative uncertainties are 2.5% to 6% and the absolute normalization uncertainty is about 4%. The few relative uncertainties that are larger than the symbol size are indicated by the error bars. The total energy spread, as determined for the experimental conditions using the Monte Carlo codes described above, decreases monotonically from 190 to 94 keV for energies from 8 to 14 MeV. The energy spread at 17 MeV is 300 keV because a higher deuterium gas pressure[2] was used at this energy. The solid curves in Fig. 3 represent Legendre polynomials fits to the data. The data points at 0° represent Wick's limit calculated using values for the total cross section obtained in experiments in the references mentioned in Sec. III A.

During the period of our ^{93}Nb measurements, tests were being conducted for adapting a special collimation apparatus loaned to TUNL by the Ballistic Research Laboratory in Aberdeen, MD. The system allows $\sigma(\theta)$ measurements to be performed at scattering angles near 0° and is described in detail in Refs. 12 and 13. Measurements were conducted at 10 MeV for ^{93}Nb(n,n) at the time of the tests. The results, normalized to current and earlier high-accuracy ^{208}Pb measurements, are included in Fig. 3 and are shown in Fig. 4 on an expanded scale. The scattering angles ranged from 1.9° to 16° for this series of measurements. The curve in Fig. 4 is the same Legendre polynomial expansion as shown in Fig. 3. The

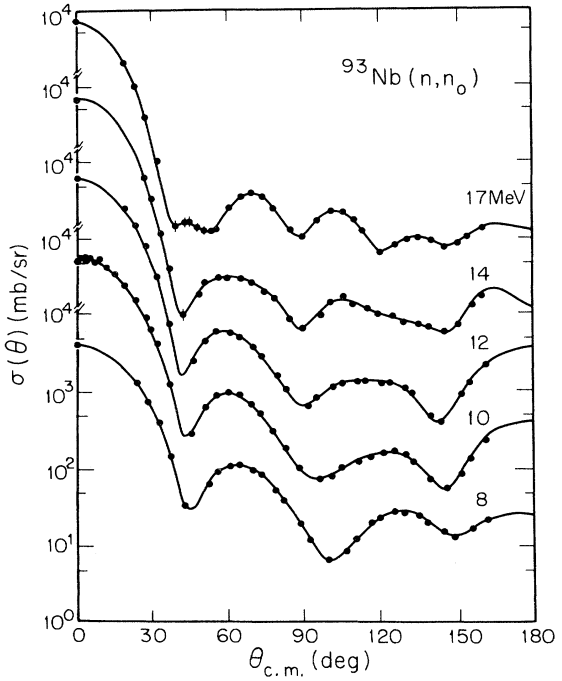

FIG. 3. Differential cross sections for elastic scattering of neutrons from ^{93}Nb. The curves are Legendre polynomial fits.

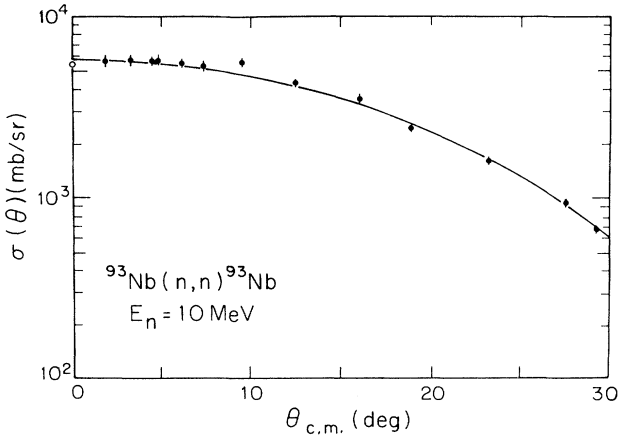

FIG. 4. Expanded view of 10-MeV data and polynomial fit to issustrate the values obtained with the small-angle measuring system. The open circle at 0° represents Wick's limit as calculated from the measured total cross section. Data for $\theta > 17°$ were obtained with the conventional detector arrangement.

dimensions of the ^{93}Nb slab and the details of error calculations are given in Ref. 13.

The final $A_y(\theta)$ data are shown in Fig. 5. The uncertainties range from less than ± 0.02 at forward angles to about ± 0.08 at some backward angles. The error bars illustrated in Fig. 5 include all uncertainties, except that of a uniform scale factor of about ± 0.03, which is attributed to uncertainties in the quench-ratio measurements and in the ^{2}H$(d,n)^3$He polarization-transfer coefficients. The curves accompanying the $A_y(\theta)$ data in Fig. 5 are derived

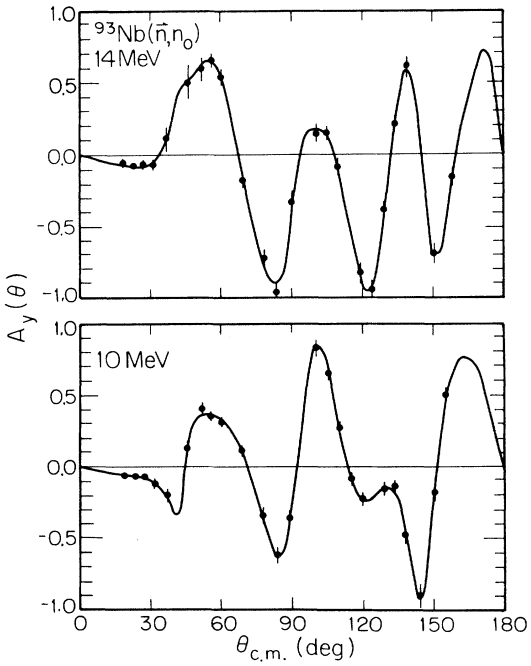

FIG. 5. Analyzing powers for elastic scattering of neutrons from ^{93}Nb. The curves are derived from expansions of the product $A_y(\theta)\sigma(\theta)$ in associated Legnedre polynomials.

from fitting an associated Legendre polynomial expansion by the product $A_y(\theta)\sigma(\theta)$, using statistical criteria to determine the optimum order for the fits. Tabulations of the $\sigma(\theta)$ and the $A_y(\theta)$ data have been transmitted to the National Nuclear Data Center at Brookhaven National Laboratory (BNL).

III. SPHERICAL OPTICAL MODEL CALCULATIONS

A. Introduction

Lagrange and Lejeune[1] have shown that the neutron-scattering cross section from ^{93}Nb is well suited for an analysis with the SOM. Furthermore, they indicate that at energies above 7 MeV the compound-nucleus contribution to elastic scattering is insignificant. A discussion of our SOM analyses of the present data follows.

The database for our analysis consists mainly of the ^{93}Nb differential cross-section and analyzing power data measured in the present work. In addition, we include the $\sigma(\theta)$ data of Etemad[14] at 7 MeV, Ferrer *et al.*[15] at 11 MeV, and Hansen *et al.*[16] at 14.6 MeV. References in the present paper to these data sets will be made using labels that indicate the respective laboratories at which the measurements were made: *AE* (Aktiebolaget Atomenergi, Studsvik, Sweden), OU (Ohio University), and LLNL (Lawrence Livermore National Laboratory). For purposes of the SOM analyses, values for the total cross section σ_T from 2.5 to 15 MeV of Foster and Glasgow[17] and from 15 to 20 MeV from ENDF/B-V (Ref. 18) are included in the data base as well. In addition, σ_T measurements[19] of the Argonne group from 1 to 4.5 MeV were also incorporated. We purposely excluded differential cross-section and analyzing power data at energies below 7 MeV in order to be free of uncertainties associated with compound nucleus scattering.

The $\sigma(\theta)$ data from 1971 of Holmqvist and Wiedling[20] at 8 MeV were not included in the analysis. A comparison of these data with the present 8-MeV data shows reasonable agreement between the two measurements, but there are noticeable differences in the three minima of the cross section. Our new data should supersede these earlier data, as techniques for Monte Carlo calculations and data acquisition have improved appreciably since the earlier measurement. A more recent set of $\sigma(\theta)$ data was reported in 1986 by Smith *et al.*[21] for the energy range from 1.5 to about 10 MeV. Their data above 8 MeV are measured in about the same detail as the present work. The agreement at 8 MeV is good in the range from 45° to their largest angle, 153°. However, for angles forward of 35° their values are about 10% higher than ours. Since none of our optical models nor the optical models of Smith *et al.* can describe these forward-angle data, we suspect that the measurement errors for these data were underestimated.

The nucleus ^{93}Nb has a $\frac{9}{2}^+$ ground state and a low-lying $\frac{1}{2}^-$ first excited state at 0.030 MeV. This large angular momentum difference inhibits inelastic scattering to this state. Since our time-of-flight spectrometer could not resolve these two groups of neutrons, we made an estimate of the inelastic cross section using the coupled channels code[22] ECIS79. The calculation followed the prescription described by Crawley and Garvey[23] for ^{27}Al(p,p') and Whisnant *et al.*[24] for ^{27}Al(n,n'). In the calculation a proton hole is coupled to the core of the nucleus ^{94}Mo. The calculated cross section indicated that the contribution from this 0.030-MeV state should be much smaller than that for elastic scattering, even in the diffraction minima. Considering that the absolute uncertainties of the present data are largest in the minima and that the data were weighted in proportion to the square of the uncertainties for the SOM searches, any residual effect of the contamination by these inelastically scattered neutrons would have little effect on the SOM analyses presented here.

For the SOM calculations, we define the OMP to be given by

$$U(r)=-V_R f(r,R_R,a_R)-iW_V f(r,R_V,a_V)+4ia_D W_D \frac{d}{dr} f(r,R_D,a_D)$$
$$+2\lambda\frac{2}{\pi}\frac{1}{r}\left[V_{\text{s.o.}}\frac{d}{dr}f(r,R_{\text{s.o.}},a_{\text{s.o.}})\mathbf{l}\cdot\mathbf{s}+iW_{\text{s.o.}}\frac{d}{dr}f(r,R_{\text{s.o.}},a_{W_{\text{s.o.}}})\mathbf{l}\cdot\mathbf{s}\right],$$

where the form factors $f(r,R_i,a_i)$ are standard Woods-Saxon functions and $R_i=r_i A^{1/3}$. Calculations were made using the search code GENOA, which originated with F. G. Perey of Oak Ridge National Laboratory. This code was modified[25] at TUNL to include a correction for the Mott-Schwinger interaction[26] between the magnetic moment of the incident neutron and the Coulomb field of the nucleus. This modification is important for our purposes, since Mott-Schwinger scattering is known to affect neutron analyzing powers significantly, particularly in the small-angle region. As is usual in optical model analyses, optimum fits were determined by minimizing the chi-squared per data point. In the analysis the $A_y(\theta)$ data were given double weighting since we were interested in obtaining a determination of the spin-orbit potential based on the inclusion of $A_y(\theta)$ data and since there are eight $\sigma(\theta)$ distributions and only two $A_y(\theta)$ distributions.

B. Spherical optical model calculations from global parameter sets

Predictions using several existing SOM parameter sets have been made for comparison to the ^{93}Nb data. The first is the phenomenological parameter set from the ^{93}Nb analysis of Lagrange and Lejeune[1] for the 10-keV to 50-MeV range. This model was derived from a database that included the following: the (n,n) differential cross-section data at 7, 8, and 11 MeV of Refs. 14, 20, and 15, respectively; the total cross sections of Ref. 17 between

2.5 and 15 MeV; the (p,p) differential cross-section data of Fulmer[27] at 22.2 MeV; the (p,n) cross-section data of Wong *et al.*[28] at 18.7 MeV and Batty *et al.*[29] at 49.4 MeV; and the (p,p) analyzing power data of Rosen *et al.*[30] at 10.5 and 14.5 MeV. The second parameter set is set A of the global analysis of Rapaport, Kulkarni, and Finlay,[31] derived through a description of neutron-scattering data for ^{40}Ca, ^{90}Zr, ^{92}Mo, ^{116,124}Sn, and ^{208}Pb over an energy range from 7 to 26 MeV. Note that neither of these studies considered $A_y(\theta)$ data for neutrons in their analyses. The final set considered is from the global parameter set of Walter and Guss[4] for the 10–80-MeV range. This model is based on both $\sigma(\theta)$ and $A_y(\theta)$ data for proton and neutron scattering from nuclei with $A \geq 54$. The database employed by Walter and Guss includes our present 10- 14- and 17-MeV $\sigma(\theta)$ data and our 10- and 14-MeV $A_y(\theta)$ data for ^{93}Nb, although this entire data set was given reduced weight in their searches because the present data were considered preliminary at that time.

The parameters for these three models are given in Table I and listed as Lagrange and Lejeune (LL), Rapaport, Kulkarni, and Finlay set A (RKF-A), and Walter and Guss (WG). It is important to note that the usual symmetry terms V_1 and W_1 appear in these potentials. We have evaluated these quantities for ^{93}Nb(n,n) and included them in the respective V_R and W_D listed in Table I. In Fig. 6 the $\sigma(\theta)$ data are compared to calculations based on the above-mentioned models. It can be seen that the WG parameters give the best representations of the data and describe the structure in the distributions extremely well (except for the angular ranges between 100° and 140° at 11 MeV and between 35° and 55° at 17 MeV). The success of the WG model is especially pleasing since this model is highly constrained by the large global database used in its derivation. (We note here that our models discussed in the next section are specifically designed for ^{93}Nb, but they still do not eliminate the deficiencies seen for the WG model in the above angular ranges.) As can be seen in Fig. 6, the predictions based on sets LL and RKF-A are in fair agreement at the lower energies but worsen as E increases, with the predictions underestimating $\sigma(\theta)$ in a manner symptomatic of excessive absorption in the OMP (see also Ref. 2).

The $A_y(\theta)$ data are compared to calculations for these sets in Fig. 7. The large negative values in the calculations near 1° are due to the Mott-Schwinger electromagnetic interaction mentioned above. The RKF-A parameters give a good representation of the $A_y(\theta)$ data. This is somewhat surprising since the database of the RKF

TABLE I. Spherical optical model parameters for ^{93}Nb.

Parameter	LL	RKF-A	WG	Set I[a]	Set II[a]
V_R (MeV)	$49.1-0.26E$	$51.51-0.31E$	$50.61-0.300E$	$50.65-0.297E$	$51.18-0.241E$
r_R (fm)	1.24	1.198	1.219	1.22	1.20
a_R (rm)	0.62	0.663	0.668	0.685	0.69
W_V (MeV)	0.0	0.0	0.0	0.0	0.0
	($E \leq 11$ MeV)	($E \leq 15$ MeV)	($E \leq 6.3$ MeV)	($E \leq 6.53$ MeV)	($E \leq 9.9$ MeV)
	$0.16E-1.76$	$0.38E-4.3$	$0.153E-0.963$	$0.182E-1.188$	$0.179E-1.75$
	($E \geq 11$ MeV)	($E \geq 15$ MeV)	($E \geq 6.3$ MeV)	($E \geq 6.53$ MeV)	($E \geq 9.9$ MeV)
r_V (fm)	1.24	1.295	1.420	1.345	1.42
a_V (fm)	0.62	0.590	0.509	0.636	0.50
W_D (MeV)	$3.40+0.41E$	$2.77+0.40E$	7.53[b]	7.30	8.00
	($E \leq 11$ MeV)	($E \leq 15$ MeV)	($E \leq 9.9$ MeV)	($E \leq 11.08$ MeV)	($E \leq 9.9$ MeV)
	$9.67-0.16E$	$12.77-0.39E$	$9.083-0.157E$	$10.25-0.266E$	$9.772-0.179E$
	($E \geq 11$ MeV)	($E \geq 15$ MeV)	($E \geq 9.9$ MeV)	($E \geq 11.08$ MeV)	($E \geq 9.9$ MeV)
r_D (fm)	1.26	1.295	1.282	1.286	1.31
a_D (fm)	0.58	0.590	0.512	0.522	0.50
$V_{s.o.}$ (MeV)	7.71	6.2	$6.004-0.015E$	$6.740-0.015E$	$6.84-0.033E$
$r_{s.o.}$ (fm)	1.12	1.01	1.103	1.13	1.14
$a_{s.o.}$ (fm)	0.47	0.75	0.560	0.511	0.50
$W_{s.o.}$ (MeV)	0.0	0.0	$0.791-0.018E$	$0.954-0.018E$	$0.741-0.009E$
$R_{W_{s.o.}}$ (fm)	0.0	0.0	1.364	1.267	1.26
$a_{W_{s.o.}}$ (fm)	0.0	0.0	0.632	0.511	0.50

[a]These SOM paramters are intended for use in the 7–20-MeV region, although they may be applicable even for energies beyond 40 MeV. However, because of the constant W_D value for energies below about 11 MeV, they are not expected to be reliable below about 7 MeV.

[b]In the WG parameter set W_D is given only for $E \geq 9.9$ MeV; for the WG predictions at lower energies W_D has been set to a constant value of 7.53 MeV, its value at $E=9.9$ MeV.

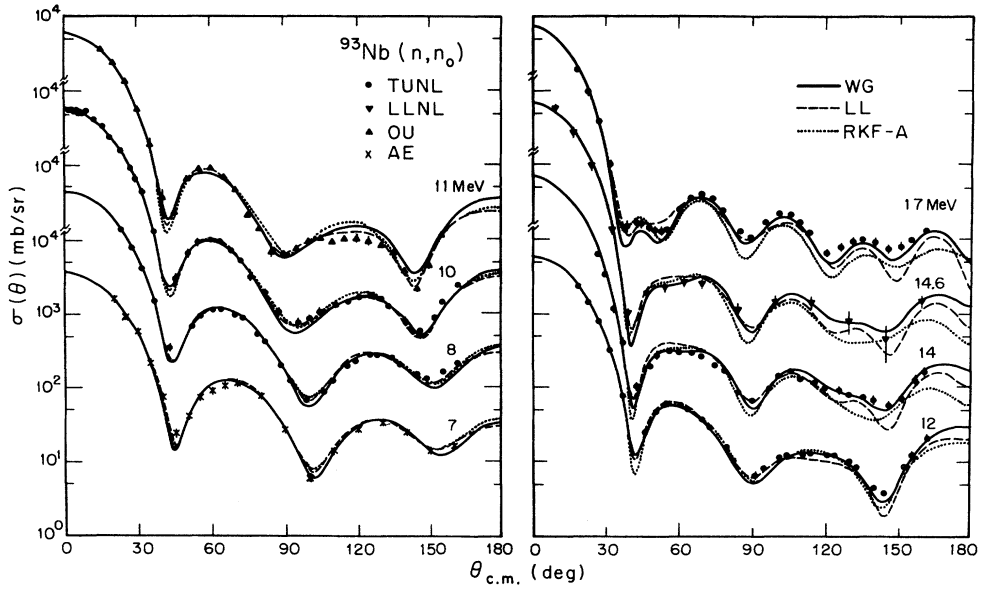

FIG. 6. Differential cross sections for elastic scattering of neutrons from ^{93}Nb. Data are from present work (TUNL), Lawrence Livermore National Laboratory (Ref. 16), Ohio University (Ref. 15), and Aktiebolaget Atomenergi (Ref. 14). Curves represent SOM calculations using previously published parameters (see text).

analysis did not include analyzing power data; these authors chose to employ the spin-orbit parameters from a 1969 global analysis of Becchetti and Greenlees,[32] which was based mainly on proton-nucleus scattering. The WG parameters, which were derived using $A_y(\theta)$ data for many nuclei, also give reasonably good predictions of the $A_y(\theta)$ data. The predictions using the LL parameters are poor for backward angles.

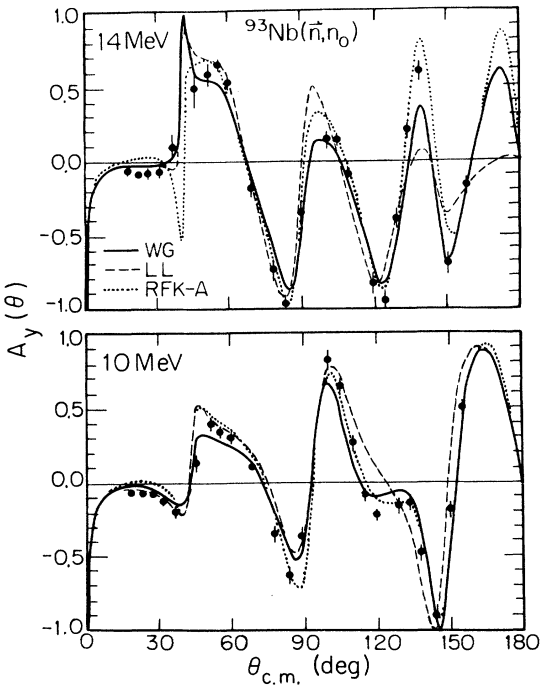

FIG. 7. Analyzing powers for elastic scattering of neutrons from ^{93}Nb. The data are from the present work. See caption of Fig. 6.

C. Spherical optical model parameter searches

In the present work several sets of SOM parameters for ^{93}Nb were derived in searches using the code GENOA. Each search had different initial parameters or different constraints. All of the derived sets have geometrical parameters that are energy-independent and potential strengths that vary linearly with energy. The volume absorptive strength W_V was set equal to zero below a specified energy. In addition, because $\sigma(\theta)$ and $A_y(\theta)$ data below 7 MeV were excluded in the analysis, it was decided to constrain the surface absorptive potential W_D to a constant value below some specified neutron energy. Thus, caution is advised in the use of the potentials reported here—one must recognize that the potentials may not be reliable at energies far from those of the present data, particularly at very low energies.

The first search used the WG parameters as the starting point. (Quite similar final parameters were also obtained using the RKF-A and the LL parameters as starting points in searches.) Unfortunately, the search converged upon a solution that had an unreasonably large energy dependences for the real and imaginary spin-orbit potentials $V_{s.o.}$ and $W_{s.o.}$. Therefore, in the second search restrictions were placed on the spin-orbit parameters. The energy dependences were fixed at the more acceptable values of $-0.015E$ for $V_{s.o.}$ and $-0.018E$ for $W_{s.o.}$ which are slopes derived in the global search of Walter and Guss that covered the 10–80-MeV energy range. The imaginary spin-orbit diffuseness $a_{W_{s.o.}}$ was also constrained to equal $a_{s.o.}$, since the optimum value

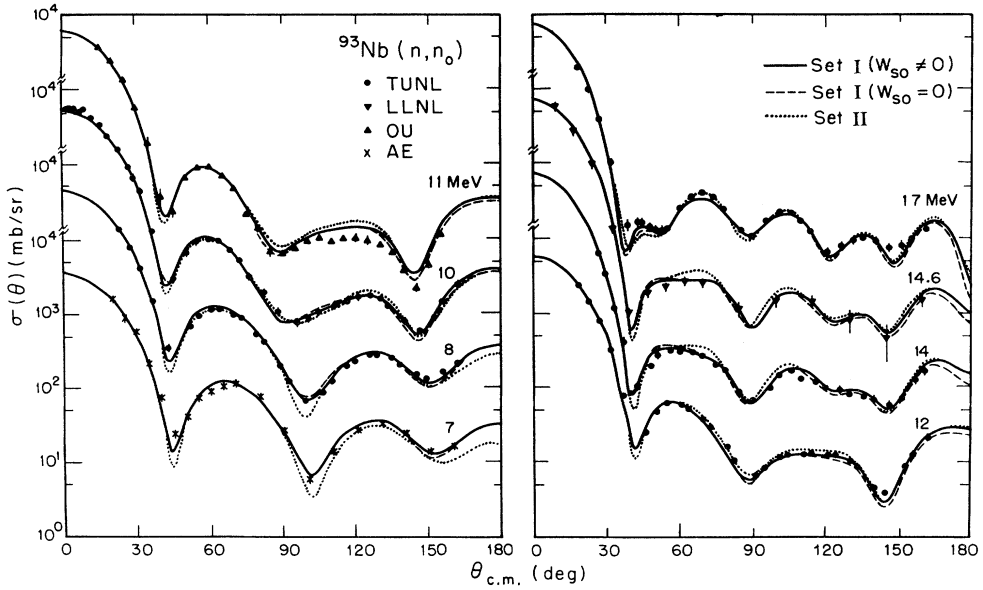

FIG. 8. Differential cross sections for elastic scattering of neutrons from ^{93}Nb. The solid curves are from calculations using the set-I parameters and the dashed curves are for the same set of parameters but with $W_{s.o.}=0$. The dotted curves are calculations that use the set-II parameters.

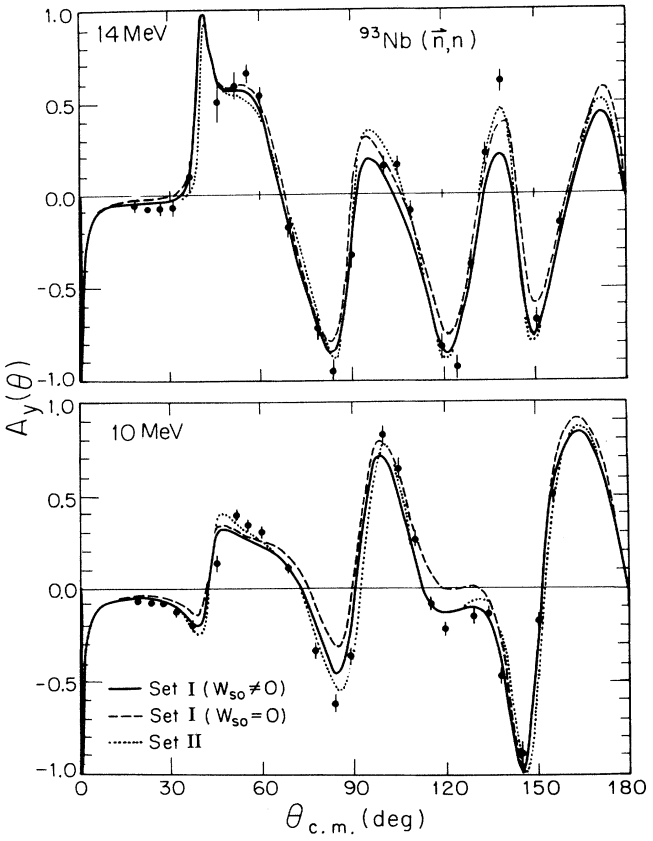

FIG. 9. Analyzing powers for elastic scattering of neutrons from ^{93}Nb. The curves use the same convention as in Fig. 8.

obtained in the initial searches was considered to be unrealistically small ($a_{W_{s.o.}} < 0.25$ fm). Searches were made to optimize the remaining parameters, and the resulting set I listed in Table I was obtained. The calculations in Figs. 8 and 9 for the set I parameters show significantly improved agreement with the data compared to the predictions from the WG parameters shown in Figs. 6 and 7, especially for the $\sigma(\theta)$ data and the 10-MeV $A_y(\theta)$ data. The calculations from these set I parameters are nearly identical to those of the earlier model that has the unreasonable spin-orbit energy dependences.

The existence of the imaginary spin-orbit term $W_{s.o.}$ deserves discussion, since this term has usually been omitted from conventional analyses of nucleon-nucleus scattering below 50 MeV. Historically, the omission of $W_{s.o.}$ has occurred in neutron-scattering analyses because $\sigma(\theta)$ is relatively insensitive to its presence and because most of the early $A_y(\theta)$ data existed for energies below 4 MeV, the energy region where compound-nucleus scattering makes it difficult to determine the spin-orbit interaction. In the present SOM analysis we found that our fit to $A_y(\theta)$ is moderately sensitive to the presence of $W_{s.o.}$ and the description of the $A_y(\theta)$ data is improved by including it. To demonstrate the sensitivity of the calculations to this term, we simply set $W_{s.o.}$ to zero in set I and calculated $\sigma(\theta)$ and $A_y(\theta)$ without changing any other parameters. As can be seen in Fig. 8, there are only small differences between the $\sigma(\theta)$ calculations with $W_{s.o.}>0$ and $W_{s.o.}=0$. The differences between the corresponding two sets of $A_y(\theta)$ calculations are more pronounced, as shown in Fig. 9.

To see if this $W_{s.o.}$ finding was symptomatic to the family of parameters in set I, we made additional SOM searches with the data base. In one case we initiated the

search with the RKF-A parameters. To avoid the problem of converging on a $W_{s.o.}$ that has too large an energy dependence, the slope was fixed at the one found in the WG model (and used in obtaining set I). In order to keep some "flavor" of the initial parameter set, the search was confined to varying only three parameters in addition to $W_{s.o.}$. The search was started with $W_{s.o.}$ set to zero. The end result after searching with eight combinations of the four parameters (with three to five iterations per search) was the following: V_R(MeV) went from 51.51 to 52.05, $V_{s.o.}$(MeV) from 6.20 to 6.61, r_D(fm) from 1.295 to 1.278, a_D(fm) from 0.590 to 0.596. The final value for the intercept of $W_{s.o.}$(MeV) at $E_n=0$ is 0.642. A somewhat similar test was made with the WG parameters. First, however, $W_{s.o.}$ was set to zero and seven parameters were optimized via several searches with many iterations. When $W_{s.o.}$ was then allowed to vary, it rapidly increased to 0.71 MeV and the total χ^2 decreased by 30%. Similar attempts were made starting $W_{s.o.}$(MeV) at 0.2, 0.4, and 0.6 and in every case the final value was around 0.7. We conclude from these exercises that within the framework of the spherical optical model, the data favor a positive $W_{s.o.}$ between 0.6 and 0.8 MeV for the energy region near 8 to 14 MeV, a finding in close agreement with TUNL observations for other nuclei.[2,33–37]

Since applied scientists perhaps will desire a parameter set which omits $W_{s.o.}$ for calculational simplicity, a parameter set was obtained from a search in which the $W_{s.o.}$ strength was held to zero. The search was initiated using the set I parameters and allowing three of these parameters to vary. The results from these searches are $V_R=49.76$ MeV, $V_{s.o.}=6.64$ MeV, and $r_D=1.30$ fm. The χ^2 is about 50% of that obtained with RKF-A (with $W_{s.o.}=0$) and about 50% greater than that for set I. The calculations look very similar to the ones in Figs. 8 and 9 with $W_{s.o.}=0$.

The total cross sections calculated from the set I parameters are shown in Fig. 10 along with the σ_T data from Foster and Glasgow[17] (2.5 to 15 MeV), from ENDF/B-V (1 to 20 MeV)[18], and from Smith *et al.*[19] (1 to 4.5 MeV). It is clear that there is excellent agreement between the data and the calculation. Even though $\sigma(\theta)$ data below 7 MeV were not considered in the search and W_D was held constant below 7 MeV, the predicted energy dependence of σ_T is quite good down to 1 MeV. Comparisons with low-energy $\sigma(\theta)$ data (properly corrected for compound-nucleus contributions) would provide a better test of the applicability of the model at low energies.

In the report on an earlier companion study of neutron scattering from ^{89}Y, $\sigma(\theta)$ and $A_y(\theta)$ data in the 8–17-MeV range are presented[2] and parametrized with the SOM. Since the data for ^{89}Y are very well described by the SOM, and ^{89}Y is a close neighbor of ^{93}Nb, an attempt was made in the present work to describe the ^{93}Nb data with a parameter set derived from the parameters for ^{89}Y. It was expected that the ^{89}Y parameter set could be adapted to describe ^{93}Nb with only minimal changes in the strength or energy dependence of the imaginary potential.

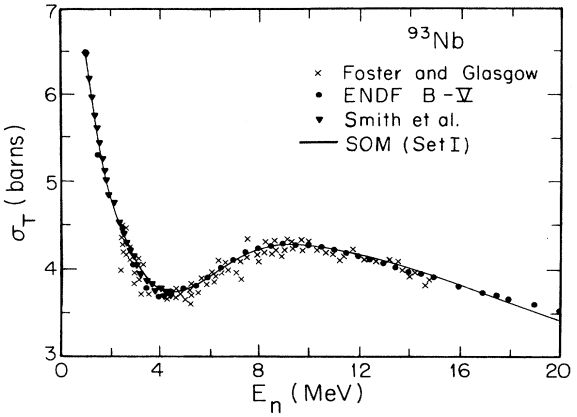

FIG. 10. Total cross sections for ^{93}Nb (Refs. 17–19) compared to calculations made using the set-I parameters of the present work.

First, it is important to recall the need to include symmetry terms in nucleon-nucleus optical potentials. It is usual in global models to parametrize part of the N and Z dependence of the real and imaginary potentials in terms of the asymmetry $\varepsilon=(N-Z)/A$. Commonly employed models, such as the RKF model, include such terms only in the central potentials V_R and W_D, while some more recent models, such as WG, include the symmetry term in the spin-orbit potential $V_{s.o.}$ as well. Empirical findings indicate that this latter term is quite small. Therefore, for the present purpose where we would like to estimate the dominant corrections for creating a ^{93}Nb parameter set from an ^{89}Y set, we ignore this latter dependence. Including the symmetry term, we have

$$V_R=(V_{00}-\alpha_R E)-\varepsilon V_1 ,$$

where

$$V_1=V_{10}-\alpha_1 E$$

and

$$W_D=W_{D0}-\alpha_D E-\varepsilon W_{D1} .$$

Using the WG parameters ($V_{10}=16.50$ MeV, $\alpha_1=0.018$, and $W_{D1}=14.94$ MeV), the respective values of εV_1 for ^{93}Nb and ^{89}Y are 1.95 MeV and 2.04 MeV; thus, we can expect the real potential V_R for ^{93}Nb to be approximately $\Delta V_1=100$ keV greater than that for ^{89}Y at any energy. (It is worth noting here that, although the slope α_R of the real potential also has a symmetry-dependent correction as well, this modification is not significant for these two nuclei, and ΔV_1 can be considered constant with energy for purposes of the present discussion.) Similarly, εW_{D1} has values of 1.77 and 1.85 MeV for ^{93}Nb and ^{89}Y, respectively; one therefore expects W_D for ^{93}Nb to be larger than W_D for ^{89}Y by an amount $\Delta W_{D1}\cong 120$ keV.

Searches on the ^{93}Nb data set were conducted, initially starting from the unmodified ^{89}Y parameters of Ref. 2. All geometrical parameters were kept fixed at their origi-

nal values throughout these searches. The effect of the volume absorptive potential W_V on the calculations is slight, since its magnitude is small in the 8–17-MeV energy range. Therefore, W_V was left unaltered in the entire search process. The parameter search was divided into two stages. In the first stage, the absorptive surface potential W_D was optimized. It was found that ^{93}Nb requires a strength for W_D that is about 1.4 MeV greater than that for ^{89}Y; this difference is a factor of 10 larger than is predicted by the εW_{D1} symmetry term of the WG model. This result is not entirely surprising, since it was already found in our earlier work[2] with ^{89}Y that the imaginary potential strength for this nucleus exhibits a behavior that is not predicted by any existing global model. In the second stage the strength of the real central potential V_R was searched upon, alone and then simultaneously with W_D. The strength of W_D did not differ from that found in the first stage. The difference in V_R obtained for the two nuclei,

$$V_R(\text{niobium}) - V_R(\text{yttrium}) \cong +150\text{keV} ,$$

has the same sign and approximate size as that predicted by the WG model ($\Delta V_1 \cong 100$ KeV). The final SOM parameters from this search procedure are listed in Table I as set II.

The SOM calculations for ^{93}Nb using the parameters of set II are shown in Figs. 8 and 9 (dotted curves). The descriptions of the $\sigma(\theta)$ data using this modified ^{89}Y parameter set are somewhat inferior to those calculated from set I, but the representation of $A_y(\theta)$ is improved. This latter observation indicates that the spin-orbit parameters reported for ^{89}Y (which also include a positive $W_{\text{s.o.}}$) are well suited to describing the $A_y(\theta)$ for ^{93}Nb as well.

Summarizing the SOM findings, we note that considering the overall fits of the combined $\sigma(\theta)$ and $A_y(\theta)$ data sets, the set-I parameters give the best description. Looking carefully at the details of the agreement in the 7–20-MeV range, one sees that these parameters permit fairly accurate representations of $\sigma(\theta)$ and σ_T, and also give reasonable representations of $A_y(\theta)$. Improved agreement for $A_y(\theta)$ can be made using set II, which is based on an ^{89}Y model. Some systematic discrepancies exist, however, between the calculations and the $\sigma(\theta)$ data at 10 and 17 MeV, and the $A_y(\theta)$ data at 10 and 14 MeV. The discrepancies in $\sigma(\theta)$ at 11 MeV may indicate a distinct problem with the Ohio University data at this energy, since similar discrepancies exist between these data and the predictions of the LL parameters and of the RKF-A parameters. At 17 MeV the discrepancies in $\sigma(\theta)$ near the first minimum are a curious feature of the data in this mass range.[2] Higher-energy data and analyses might be instructive in resolving the cause of this discrepancy.

As for the $A_y(\theta)$ data, it is quite possible that the SOM is simply not a suitable model for describing the fine details of these data and that using a different approach would improve the predictions. If one postulates strong coupling of one or more of the excited states to the ground state, then coupled-channel calculations might give some insight, but the interpretation of the validity of such calculations is hampered by the absence of inelastic-scattering data for ^{93}Nb. Such data are extremely difficult to obtain with present neutron spectroscopy equipment, as there are approximately 30 low-lying states with excitation energies below 2 MeV.

Finally, we note that Hansen *et al.*[16] have obtained a good description of their $\sigma(\theta)$ data at 14.6 MeV using the microscopic model of Jeukenne, Lejeune, and Mahaux (JLM).[38] However, they did not publish $A_y(\theta)$ predictions that could be compared to our data. As mentioned in the introduction, additional calculations are currently underway at LLNL with Hansen and Dietrich[4] to determine the capability of the JLM model and other microscopic models to reproduce the analyzing power data reported here.

IV. SUMMARY AND CONCLUSIONS

Differential cross sections and analyzing powers for ^{93}Nb(n,n) have been measured in the energy range between 8 and 17 MeV. Several descriptions of the data have been made using the spherical optical model; quite good results are achieved using potentials having constant geometry parameters and potential strengths that vary linearly with energy. A comparison of the data to two existing global SOM parameter sets has also been made, and reasonable predictions were obtained for much of the $\sigma(\theta)$ and $A_y(\theta)$ angular distributions with one (WG). In addition, quite good agreement has been achieved with a parameter set derived at TUNL for ^{89}Y(n,n) by only introducing a small change in the surface absorptive potential.

The $A_y(\theta)$ data indicate that when an SOM with Woods-Saxon form factors is used to describe the data, there is a desire for the spin-orbit potential to have an imaginary part with a small positive strength ($W_{\text{s.o.}} \leq +1$ MeV). A term of this magnitude and sign is comparable to values obtained in several earlier TUNL studies.

In the last five years major breakthroughs have been made for connecting the nucleon-nucleus potential for elastic scattering to the potential for bound states in a consistent way using the dispersion relation. Many analyses have been done for the $n+^{40}$Ca and $n+^{208}$Pb with good successes in fitting observables for -20 MeV $< E_n <$ 80 MeV. (For example, illustrations are given in Ref. 39.) The work for intermediate-mass nuclei is quite sparse. We are presently performing such an analysis of the scattering data reported here along with σ_T data from 1 to 80 MeV to determine if such a model can give a better representation of the data than the one obtained here that uses more conventional energy dependences on the parameters.

ACKNOWLEDGMENTS

We gratefully acknowledge the participation of H. G. Pfützner and G. Tungate in the measurements, and discussions with V. A. Madsen and P. D. Kunz regarding calculations for the inelastic scattering contaminant. This work was supported by the U.S. Department of Energy, Office of High Energy and Nuclear Physics, under Contract No. DE-AC05-76ER01067.

*Present address: John E. Edwards Accelerator Laboratory, Ohio University, Athens, OH 45701.
†Present address: Los Alamos National Laboratory, Los Alamos, NM 87545.
‡Present address: Bowman Gray School of Medicine, Winston Salem, NC 27103.

[1]Ch. Lagrange and A. Lejeune, Phys. Rev. C **25**, 2278 (1982).
[2]G. M. Honoré, R. S. Pedroni, C. R. Howell, H. G. Pfützner, R. C. Byrd, G. Tungate, and R. L. Walter, Phys. Rev. C. **34**, 825 (1986).
[3]R. L. Walter and P. P. Guss, in *Nuclear Data for Basic and Applied Science,* Proceedings of the International Conference, Santa Fe, New Mexico, 1985, edited by P. G. Young, R. E. Brown, G. F. Auchampaugh, P. W. Lisowski, and L. S. Stewart (Gordon and Breach, New York, 1986), p. 1079; see also R. L. Walter, in *Neutron-Nucleus Collisions—A Probe of Nuclear Structure, Burr Oak State Park, Ohio, 1984,* Proceedings of the Workshop, AIP Conf. Proc. No. 124, edited by J. Rapaport, R. W. Finlay, S. M. Grimes, and F. S. Dietrich (AIP, New York, 1985), p. 53.
[4]L. Hansen, F. S. Dietrich, and R. L. Walter, Bull. Am. Phys. Soc. **33**, 1570 (1988).
[5]S. M. El-Kadi, C. E. Nelson, F. O. Purser, R. L. Walter, A. Beyerle, C. R. Gould, and L. W. Seagondollar, Nucl. Phys. **A390**, 509 (1982).
[6]W. Tornow, E. Woye, G. Mack, C. E. Floyd, K. Murphy, P. P. Guss, S. Wender, R. C. Byrd, R. L. Walter, and H. Leeb, Nucl. Phys. **385**, 376 (1982).
[7]G. G. Ohlsen, J. L. McKibben, G. P. Lawrence, P. W. Keaton, and D. D. Armstrong, Phys. Rev. Lett. **27**, 599 (1971).
[8]R. C. Byrd, P. W. Lisowski, W. Tornow, and R. L. Walter, Nucl. Phys. **A404**, 29 (1983); see also W. Haeberli, in *Fast Neutron Physics,* edited by J. B. Marion and J. L. Fowler (Wiley, New, 1963), p. 1390.
[9]J. C. Hopkins and G. Breit, Nucl. Data Tables **A9**, 137 (1971).
[10]H. H. Hogue, TUNL computer code EFFIGY (unpublished).
[11]E. Woye, W. Tornow, G. Mack, C. E. Floyd, P. P. Guss, K. Murphy, R. C. Byrd, S. A. Wender, R. L. Walter, T. B. Clegg, and W. Wylie, Nucl. Phys. **A394**, 139 (1983).
[12]W. Bucher, C. E. Hollandsworth, and R. Lamoreaux, Nucl. Instrum. Methods **111**, 237 (1973).
[13]R. S. Pedroni, Ph.D. dissertation, Duke University (1986).
[14]M. A. Etemad, Aktiebolaget Atomenergi Report AE-482 (Studsvik, Sweden), 1973.
[15]J. C. Ferrer, J. D. Carlson, and J. Rapaport, Nucl. Phys. **A275**, 325 (1977).
[16]L. F. Hansen, F. S. Dietrich, B. A. Pohl, C. H. Poppe, and C. Wong, Phys. Rev. C **31**, 111 (1985).
[17]D. G. Foster, Jr. and D. W. Glasgow, Phys. Rev. C **3**, 576 (1971).
[18]ENDF/B-V, available from National Nuclear Data Center, Brookhaven National Laboratory.
[19]A. B. Smith, D. Smith, and R. Howerton, Argonne National Laboratory Report ANL/NDM-88, 1985.
[20]B. Holmqvist and T. Wiedling, Aktiebolaget Atomenergi Report AE-430 (Studsvik, Sweden), 1971.
[21]A. B. Smith, P. T. Guenther, and R. D. Lawson, Nucl. Phys. **A455**, 344 (1986).
[22]J. Raynal, ECIS79 (unpublished).
[23]G. M. Crawley and G. L. Garvey, Phys. Rev. **167**, 1070 (1968).
[24]C. S. Whisnant, J. H. Dave, and C. R. Gould, Phys. Rev. C **30**, 1435 (1984).
[25]C. E. Floyd, Jr., Ph.D. dissertation, Duke University (1981).
[26]J. Schwinger, Phys. Rev. **73**, 407 (1948).
[27]C. B. Fulmer, Phys. Rev. C **125**, 631 (1962).
[28]C. Wong, J. D. Anderson, J. W. McClure, B. A. Pohl, and J. J. Weslowski, Phys. Rev. C **5**, 158 (1972).
[29]C. J. Batty, B. E. Bonner, E. Friedman, L. E. Williams, A. S. Clough, and J. B. Hunt, Nucl. Phys. **A116**, 643 (1968).
[30]L. Rosen, J. G. Beery, A. S. Goldhaber, and E. H. Auerbach, Ann. Phys. **34**, 96 (1965).
[31]J. Rapaport, V. Kulkarni, and R. W. Finlay, Nucl. Phys. **A330**, 15 (1979).
[32]F. D. Becchetti and G. W. Greenlees, Phys. Rev. **182**, 1190 (1969).
[33]J. P. Delaroche, C. E. Floyd, P. P. Guss, R. C. Byrd, K. Murphy, G. Tungate, and R. L. Walter, Phys. Rev. C **28**, 1410 (1983).
[34]C. E. Floyd, P. P. Guss, R. C. Byrd, K. Murphy, R. L. Walter, and J. P. Delaroche, Phys. Rev. C **28**, 1498 (1983).
[35]R. L. Walter, W. Tornow, P. P. Guss, and J. P. Delaroche, in *Neutron-Nucleus Collisions-A Probe of Nuclear Structure-1984, Burr Oak State Park, Ohio,* Proceedings of the Workshop, AIP Conf. Proc. No. 124, edited by J. Rapaport, R. W. Finlay, S. M. Grimes, and F. S. Dietrich (AIP, New York, 1985), p. 312.
[36]G. M. Honoré, Ph.D. dissertation, Duke University (1986).
[37]G. M. Honoré, W. Tornow, C. R. Howell, R. S. Pedroni, R. C. Byrd, R. L. Walter, and J. P. Delaroche, Phys. Rev. C **33**, 1129 (1986).
[38]J. P. Jeukenne, A. Lejeune, and C. Mahaux, Phys. Rev. C **16**, 80 (1977).
[39]C. H. Johnson, D. J. Horen, and C. Mahaux, Phys. Rev. C **36**, 2252 (1987), and references therein.